

Comparative study of singlewalled, multiwalled, and branched carbon nanotubes melt mixed in different thermoplastic matrices

Beate Krause¹, Carine Barbier¹, Karina Kunz¹, Petra Pötschke¹

¹Leibniz-Institut für Polymerforschung Dresden e.V. (IPF), Hohe Str. 6, 01069 Dresden, Germany, poe@ipfdd.de

Abstract

In this contribution, three different types of CNTs, namely single-walled (SWCNT), multi-walled (MWCNT) and branched MWCNTs were melt mixed in amounts of 0.1 – 10 wt.-% in polypropylene (PP), polycarbonate (PC) and poly(vinylidene fluoride) (PVDF) using a small-scale microcompounder. The filler dispersion of compression-moulded samples was characterized using light and electron microscopy, and the electrical and thermal properties were measured. The lowest electrical percolation thresholds were found for composites of PP/SWCNT, PP/branched MWCNT and PC/branched MWCNT, which percolated already at <0.1 wt.-% CNT loading. Low values of electrical volume resistivity of about 3 Ohm·cm (PVDF), 7 Ohm·cm (PP) and 2 Ohm·cm (PC) could be reached when loading with 2 wt.-% branched MWCNT. A homogeneous dispersion in the macro- and microlevel was observed especially for composites containing branched MWCNTs. For all CNT types, a matrix nucleation effect was found in PP and PVDF using differential scanning calorimetry.

1. Introduction

Addition of carbon nanotubes (CNTs) is a common way of achieving electrically conductive polymer materials while also improving other properties [1-4]. The enhanced properties are based on the exceptional mechanical [5], thermal [6-8] and electrical [9] properties of CNTs. The electrical properties of different melt mixed polymer/CNT composites have been already widely studied, and depending on the type of matrix polymer, type of CNTs, and melt mixing conditions, quite different percolation thresholds were found [4]. The shaping conditions (in most cases compression or injection molding) can also strongly influence the state of secondary agglomeration of the nanotubes, thereby influencing the measured conductivities and the percolation threshold [1]. Thus, a rigorous comparison of different studies is not possible. Nevertheless, some results for types of polymers under investigation in this study are discussed below.

One of the most widely used low-cost thermoplastic mass polymers is partially crystalline polypropylene (PP), which therefore is a potential candidate for property modification by the addition of CNTs. Even if PP has a very low polarity [10] and is expected to have weak interactions with CNTs, hindering good CNT dispersion, PP composites containing CNTs have been of increasing interest in the last few years and are also already important for industrial applications, e.g. as a material for external car body parts that are electrostatically paintable. The electrical properties of different melt-mixed PP-CNT composites have been already widely studied. For example, Seo et al. [11] reported electrical percolation between 1 and 2 wt.-% for melt-mixed composites of PP/ MWCNT (producer Honam Chem.Co.). Electrical percolation between 0.5 and 2 wt.-% was reported for melt mixed PP/MWCNT composites (NC7000™) by Szentes et al. [12]. Additionally, the thermal conductivity (measured by a hot disk method) increased from 0.24 W/(m·K) for pure PP up to 0.33 W/(m·K) for PP/ 5 wt.-% NC7000™. For melt-mixed PP composites filled with MWCNT

NC7000™ or MWCNT Baytubes C150P, Müller et al. [13] reported electrical percolation at 0.5 wt.-% and 1-2 wt.-%, respectively. Zhong et al. [14] obtained electrical percolation between 2 and 3 wt.-% for melt-extruded PP/MWCNT Baytubes C150P composites, and Hwang et al. [15] found a similar percolation range for melt-extruded PP/MWCNT NC7000™ composites produced via a masterbatch dilution technique. When using maleic anhydride-modified PP, electrical percolation of MWCNT NC7000™ was achieved at 1 wt.-% and occurred at about the same concentration when using ball-milled NC7000™, as reported by Menzer et al. [16]. Mičušík et al. [17] investigated the electrical percolation of PP/MWCNT composites prepared by the dilution of a Hyperion masterbatch containing 20 wt.-% MWCNT using PPs with different melt viscosity and found electrical percolation thresholds between 1.1 and 2.0 wt.-% MWCNT. Andrews et al. [18] conducted a study on the formation of PP/MWCNT (self-synthesized) composites by shear mixing and reported a low electrical percolation threshold of 0.05 vol.-% (approx. 0.14 wt.-%). Fewer studies of electrical percolation are available for PP with SWCNTs. For example, Narimani et al. [19] described a percolation threshold near 1 wt % (SWCNTs from Iljin Nanotech Co) and Krause et al. [20] reported an extremely low percolation threshold in the range of 0.075-01 wt.-% when using SWCNT of the type Tuball™ (OCSiAl).

CNTs are also reported to modify the thermal properties of PP based composites. For example, Mazov et al. [21] noted a 148% increase in thermal conductivity (relative to pure PP) when PP/4 wt.-% MWCNT composites were formed by a coagulation precipitation technique combined with melt extrusion. The melting and crystallization behavior of PP/MWCNT [22] as well as PP/SWCNT [20, 23-25] composites was also studied by different researchers, who generally observed that CNTs had a nucleating effect that results in an increase of the crystallization temperature.

Another interesting polymer is amorphous polycarbonate (PC), which has versatile engineering applications, such as housings and helmets. PC has a much higher polarity than nonpolar polyolefins [10] and is known to have good interactions with CNTs due to the aromatic rings in its chemical structure. Numerous publications [26-36] focus on melt-mixed PC/MWCNT composites and discuss, among other properties, their electrical properties and CNT dispersion. Electrical percolation thresholds between 0.2 and 2 wt.-% were described, depending of the MWCNT and PC types as well as mixing device and conditions [26-31, 33, 36-41]. Kasaliwal et al. [26] studied the influence of melt mixing conditions on CNT dispersion (MWCNT Baytubes[®] C150HP) on the macro- and nanoscale and on electrical properties. With increasing mixing energy input, the number of remaining CNT agglomerates decreased, and the values of electrical volume resistivity were reduced. Pegel et al. [36] compared the electrical properties and CNT dispersion of three different industrially available MWCNT types in PC. They concluded that CNT dispersion and distribution in the polymer melt strongly depends on the dispersability of the as-received MWCNT material itself and the strength of nanotube agglomerates. Electrical percolation was much lower for samples with higher dispersability, which was studied using the sedimentation behavior of aqueous MWCNT dispersions. Similar correlations between CNT dispersability and electrical percolation threshold were also found for other polymer matrices, for example, polyamide 66/CNT composites reported by Krause et al. [42]. Another study presented by Castillo et al. [33] compared the electrical and mechanical properties of PC-based composites with five different commercially available MWCNTs (SWeNT SMW-100, Nanocyl NC7000[™], Baytubes C150P, Continental Carbon MWCNT, Hyperion Masterbatch). In accordance with the percolation theory, with increasing aspect ratio of the nanotubes, the threshold concentration for electrical percolation decreases and varied between 0.28 and 0.60 wt.-%,

In contrast to PP/CNT and PC/CNT composites, there have been few studies of melt-mixed poly(vinylidene fluoride) (PVDF)/CNT composites. PVDF is also a partially crystalline polymer, however with a polarity much higher than PP and slightly higher than PC [10]. Ke et al. [43] reported electrical percolation thresholds of 0.53 wt.-% for non-modified MWCNTs Nanocyl™ NC3150 and 0.82 wt.-% for carboxyl-functionalized Nanocyl™ NC3151. Electrical percolation between 1 and 2 wt.-% was shown by Ameli et al. [44] for PVDF composites filled with nitrogen-doped MWCNTs (laboratory synthesized). Arjmand et al. [45] described for PVDF composites containing MWCNTs (laboratory synthesized) percolation at around 0.4 wt.-%. For MWCNTs having diameters of 10–20 nm and lengths of about 30 μm (Chengdu, P.R. China), Ke et al. [46] reported electrical percolation between 2 and 3 wt.-%, whereas Georgousis et al. [47] found percolation at 1-1.25 wt.-% for MWCNT NC7000™ and Sun et al. [48] reported percolation at contents of MWCNT NC7000™ below 2 wt.-%.

For achieving electrical conductivity in insulating polymer matrices, formation of a network of the CNTs in the polymer matrix is necessary, whereby electron hopping and tunneling processes between neighboring nanotubes also can contribute to electrical conduction. Branched CNTs (b-CNTs) having a web-like nanotube arrangement (2D or even 3D structures) have been studied in addition to linear single- and multiwalled CNT as carbon-based fillers for facilitating such network formation in thermoplastic matrices. Different methods for synthesizing branched CNTs are described in literature, e.g. the template method [49], CNT welding method [50-52], solid fiber carbonization [53], unzipping of MWCNTs [54], as well as several chemical vapor deposition based methods [55-58]. It is expected that the branched structure of b-CNTs improves the conductive network formation ability, as junctions and crossings of nanotubes are already present in the filler material. The charge transfer along junctions occurs without any contact resistance whereas at crossings a contact

resistance must be overcome. Thus, lower charge losses occur in networks formed of branched CNTs compared to networks containing linear CNTs. The interaction and load transfer between branched CNTs and the polymer matrix can be largely promoted due to the existence of side branches in b-CNTs. These side branches may strongly perturb the mobility of polymer chains in the vicinity of the reinforcements, leading to improved mechanical properties [59]. Liu et al. [59] simulated the addition of structured CNTs to polyethylene-based composites, resulting in ultra-strong nanocomposites enabled by the drastically improved interfacial strength between the reinforcement and the matrix. The interfacial strength can be significantly affected by the molecular weight of the matrix polymer as well as the geometry of the branched CNTs (number of branching points, length of branches, angle between branches). Simulations and pull-out investigations have shown that branched fibers can increase interfacial bonding [54, 60-62].

In present study, we report the preparation and characterization of polymer composites based on a new type of branched MWCNTs and compare with typical MWCNT and SWCNT materials to verify that branched CNTs impart improved electrical properties. Three polymer matrices, PP, PC and PVDF were selected as examples for amorphous polymers (PC) and partially crystalline polymers with low polarity (PP) and with higher polarity (PVDF). The morphology of the CNT materials was characterized by SEM and TEM and the electrical conductivity of the CNT powders was measured. The electrical resistivity, thermal conductivity, thermal properties, and filler macrodispersion of composites melt-mixed on a small-scale were characterized and are discussed in the context of related results in the literature.

2. Experimental Section

As the PP matrix, the homopolymer Moplen HP400R from LyondellBasel (melt flow index 25 g/min @ 230°C/2.16 kg) was used. As PC, Makrolon 2600 from Bayer MaterialScience (melt flow rate 13 g/10 min @ 300°C/1.2 kg) was applied. The PVDF matrix was Kynar720 from Arkema (melt volume rate 10 cm³/10 min @ 230°C/5 kg).

As the branched MWCNTs (b-MWCNTs), Carbon NanoStructure (CNS) flakes covered with either polyethylene glycol (CNS-PEG) or polyurethane (CNS-PU) were supplied by Applied NanoStructured Solutions LLC (Baltimore, USA). The CNS nanotubes have mean diameters of 14±4 nm, which was determined by TEM. According to the supplier, these nanotubes have an average number of 4 walls, average length of 70 μm (calculated mean aspect ratio 5000), a purity of >97%, and a bulk density of 0.135 g/cm³. In the special preparation process, a structure of a multitude of branched and entangled MWCNTs was created. According to the supplier, coating the surfaces of carbon nanotubes with polyethylene glycol (PEG) or polyurethane (PU) enhances the wettability of CNS by non-polar polymers like PP or polar polymers like PVDF, respectively, in order to improve the filler dispersion. The effectiveness of the use of PEG in dispersing MWCNTs in polyolefinic matrices has been demonstrated in the work of Müller et al. [63], who described the approach of using PEG as a dispersant additive during small-scale compounding of polyethylene/MWCNT composites. The content of PEG or PU on the CNS surface is about 5 wt.-% (determined using TGA analysis). A comparison of CNS-PEG and CNS-PU was only performed for the PVDF-based composites. For comparison, commercially available SWCNTs Tuball™ from OCSiAl S.a.r.l. (Luxembourg, Luxembourg) having a mean diameter of 1.6 nm and length exceeding 5 μm [20] (calculated mean aspect ratio 3100) as well as MWCNTs Nanocyl™ NC7000™ from Nanocyl, S.A. (Sambreville, Belgium) having diameters of around 10 nm and a mean length of 1.3 μm [64] (calculated mean aspect ratio 130) were used. Before mixing, the CNT

materials, PC and PVDF were dried at 120 °C (CNT, PC) or 80 °C (PVDF) under vacuum overnight in order to remove the moisture content.

Melt mixing of the composites was performed in a small-scale, conical, twin-screw microcompounder (Xplore DSM 15) having a volume of 15 ccm. The conditions were selected according to previous studies and were different for each kind of polymer. For PP-based composites, a mixing temperature of 210 °C, a rotation speed of 250 rpm and mixing time of 5 min were used. These melt mixing conditions are comparable to those used in refs. [20, 65]. The melt compounding of PC-based composites was performed at 280 °C, 250 rpm, and 5 minutes mixing time [38], whereas the PVDF-based composites were melt mixed at 210 °C, 200 rpm, and 10 min according to [66].

The electrical conductivity of the CNT powders was measured on as-grown material following the procedure described in ref. [67] at a pressure of 30 MPa.

The structure of the carbon nanotube material was studied by transmission electron microscopy (TEM) using a Zeiss Libra120. The CNS-PEG material was dispersed in chloroform in an ultrasonic bath for 3 minutes. A drop of freshly prepared dispersion was placed on a TEM grid covered with carbon [64].

Morphological characterization of the CNT powders and the cryo-fractured composites was performed using scanning electron microscopy (SEM) by means of a Carl Zeiss Ultra plus microscope. Before imaging, the composite strands were cryo-fractured in liquid nitrogen, and the surfaces were coated with 3 nm platinum.

To evaluate macrodispersion of the filler within the composites by transmission light microscopy (LM), the extruded strands were first cut into thin sections with a thickness of 5 μm using a Leica RM2265 microtome at room temperature and then were fixed on glass slides using Aquatex. The LM investigations were performed using an Olympus BX53M microscope combined with an Olympus DP71 camera. The agglomerate area ratio, A/A_0 , was

calculated as the ratio between the area of agglomerates with equivalent agglomerate diameters $> 5 \mu\text{m}$ (i.e. area $> 19.6 \mu\text{m}^2$) and entire imaged area (0.58 mm^2). At least 10 sections were analyzed for each sample, and the standard deviation is reported.

To prepare the samples for electrical characterization, the composites were compression molded using a PW40EH (Otto-Paul-Weber GmbH, Germany) press to sheets having a diameter of 60 mm and a thickness of 0.5 mm. PP composites were compression molded at $210 \text{ }^\circ\text{C}$ for 2 min [20, 65], PC composites at $280 \text{ }^\circ\text{C}$ for 1 min [38], and PVDF composites at $200 \text{ }^\circ\text{C}$ for 2.5 min [66]. The electrical volume resistivity of the composites was measured using two different configurations, depending on the resistivity of the samples. For samples with high resistivity, the compression-molded plates were characterized using a Keithley 8009 Resistivity Test Fixture combined with a Keithley electrometer E6517A. For samples with lower resistivity ($< 1\text{E}7 \text{ Ohm cm}$), rectangular strips ($30 \times 4 \text{ mm}^2$) were cut from the plates and characterized using a 2-point test fixture, combined with Keithley electrometer E6517A or Keithley DMM2001 multimeter.

Differential scanning calorimetry (DSC) was performed using a TA-Instruments Q2000 in the temperature range of $-80 \text{ }^\circ\text{C}$ to $200 \text{ }^\circ\text{C}$ at a scan rate of $\pm 10 \text{ K/min}$. The melting temperature observed in the second heating scan is reported. For calculating the crystallinity, α , a value of 207 J/g was used for 100% crystalline PP [68] and of 105 J/g for 100% crystalline PVDF [69].

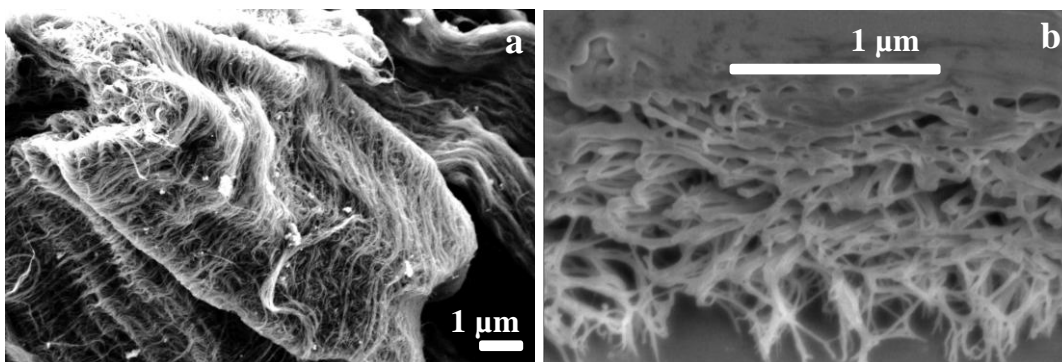
Measurements of the thermal conductivity were performed on compression-molded plates (diameter 12.5 mm, thickness 2 mm) using a light flash apparatus, LFA 447 NanoFlash (Netzsch-Gerätebau GmbH, Selb, Germany), at 25°C . Mean values were calculated from three measurements.

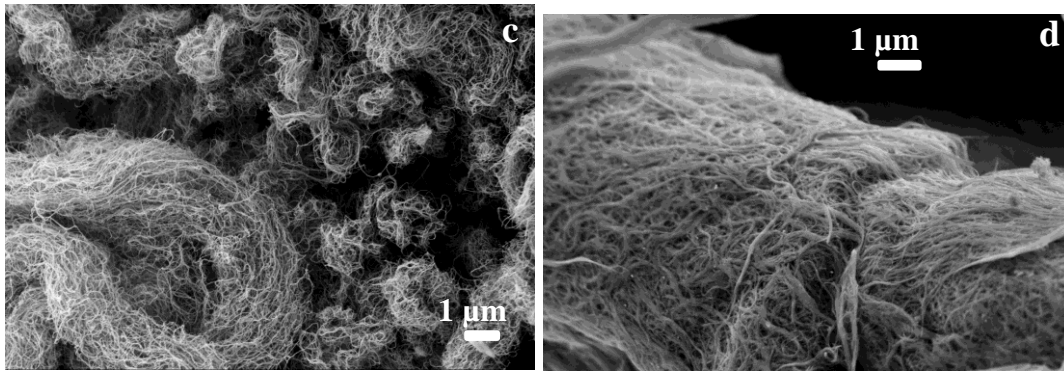
3. Results and Discussion

3.1. CNT morphology

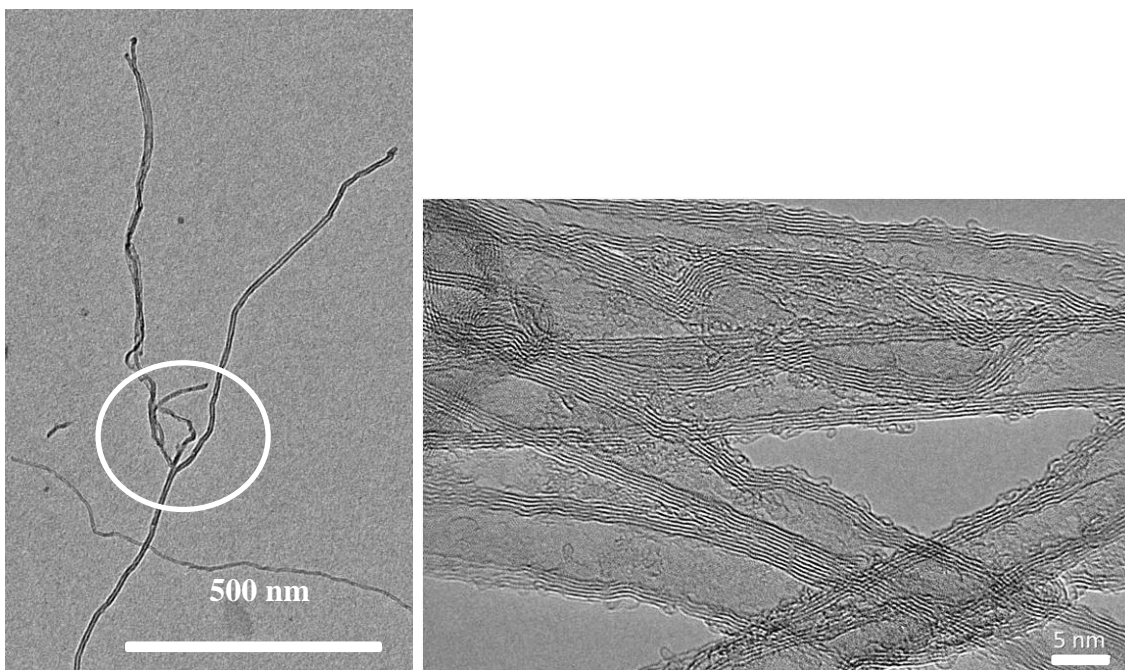
The morphology of the different CNT materials was studied using SEM, presented in Figure 1. The as-received powder of CNS-PEG has a web-like structure with yarn-like bundles of relatively long nanotubes (Fig. 1a). In Fig. 1b the branched structure of CNS-PEG is shown at lower magnification. The MWCNT type of NC7000TM shows a yarn-like structure (Fig. 1c), and for SWCNT TuballTM, bundles are visible (Fig. 1d). The TEM images in Figure 2 confirm that the CNS material contains multiwalled carbon nanotubes with low diameters. The branched structures are also visible at both magnifications. This branched structure differs significantly from the linear structures shown in the micrographs of SWCNTs TuballTM (see Fig. 1 in [20]) and MWCNTs NC7000TM (see Figure 2a in [70]).

The electrical conductivity of the CNS-PEG and CNS-PU powder was determined to be 33 S/cm and 28 S/cm, respectively. These values are slightly higher than values measured for other MWCNTs (4-30 S/cm) [44, 67, 71]. The electrical conductivity of powders of SWCNTs TuballTM and MWCNTs NC7000TM was determined to be 14 S/cm [20] and 15 S/cm [67], respectively.





Figures 1 – SEM micrographs of as-received CNT powders: (a, b) CNS-PEG, (c) NC7000[™], and (d) Tuball[™]

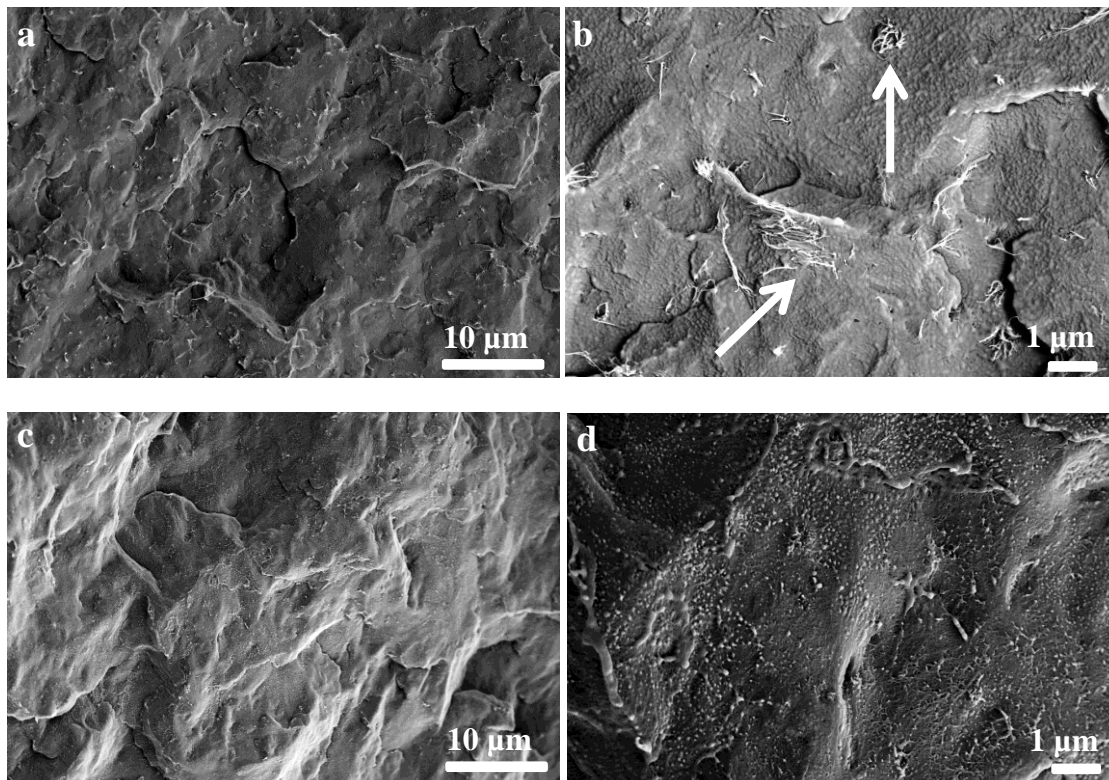


Figures 2 – TEM images of CNS-PEG

3.2 CNT dispersion in melt-mixed composites

The dispersion of CNTs was characterized in more detail for the PP composites, and SEM micrographs of the cryo-fractured surfaces of the composites filled with 1 wt.-% b-MWCNT CNS-PEG, MWCNT NC7000[™], and SWCNTs Tuball[™] are presented in Figure 3.

The SEM micrographs of the melt mixed PP/CNS-PEG composites show a good dispersion and homogeneous distribution of CNS-PEG. No large remaining agglomerates can be found (Fig. 3a), but some loosely packed, weblike structures are still seen (indicated by arrows in Fig. 3b). The nanotubes are relatively long ($>1\ \mu\text{m}$) and are well embedded in the PP matrix. For PP/NC7000™ composites, CNTs are only visible as white dots and have a relative homogeneous distribution (Fig. 3c, d). Very long, individual CNT structures and no agglomerates were observed on the cryo-fractured surface of the PP/Tuball™ composite (Fig. 3e, f). The measured CNT thicknesses indicate that the observable Tuball™ nanotubes are mostly bundled, but their distribution is quite homogeneous. The longer nanotube parts seen in the cryo-fractures indicate that these tubes are longer after processing or are not as well embedded than the MWCNTs.



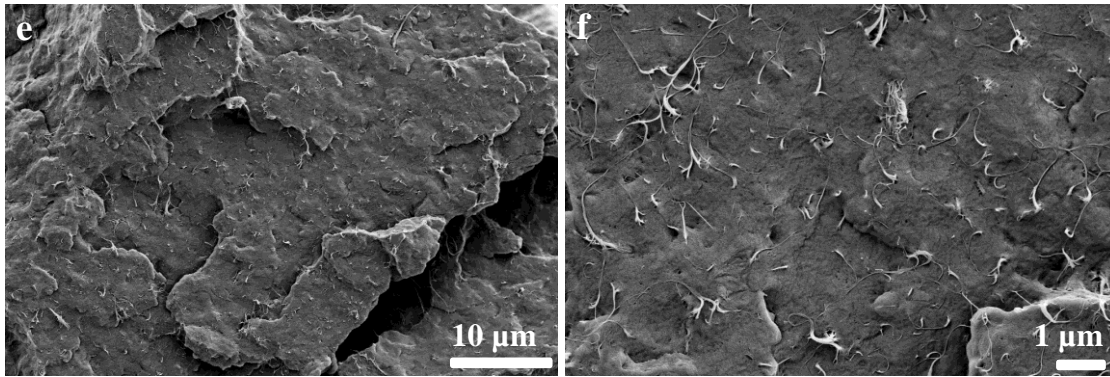
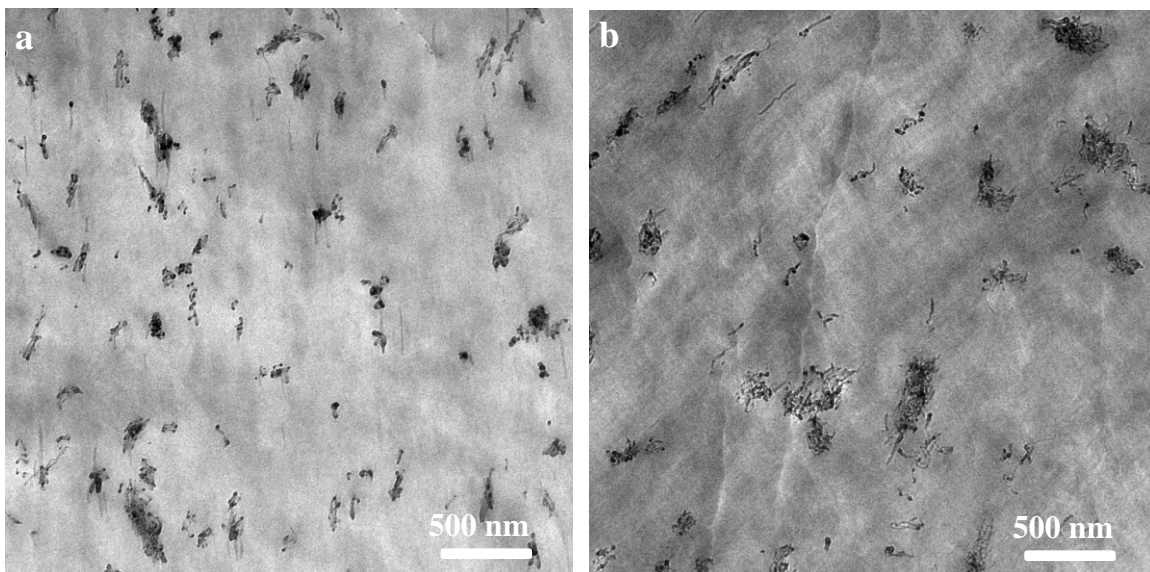


Figure 3 – SEM images of cryo-fractured surfaces of PP composite strands containing 1 wt.-% of the different fillers: (a, b) CNS-PEG, (c, d) NC7000TM and (e, f) TuballTM

The nanodispersion of CNTs in the PVDF composites was investigated in more detail by TEM, shown in Figure 4. For the PVDF composite with 1 wt.-% CNS-PEG, many individual nanotubes and very small agglomerates were homogeneously distributed (Fig. 4a). In contrast, NC7000TM nanotubes are primarily arranged as small agglomerates, and only a low number of individual CNTs are visible (Fig. 4b). TEM micrograph of PVDF/SWCNT TuballTM composites shows a high number of separate CNT (bundles) that are homogeneously distributed (Fig. 4c).



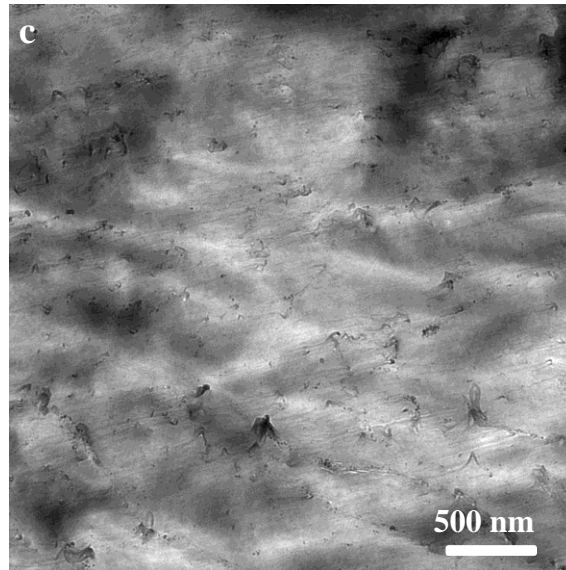
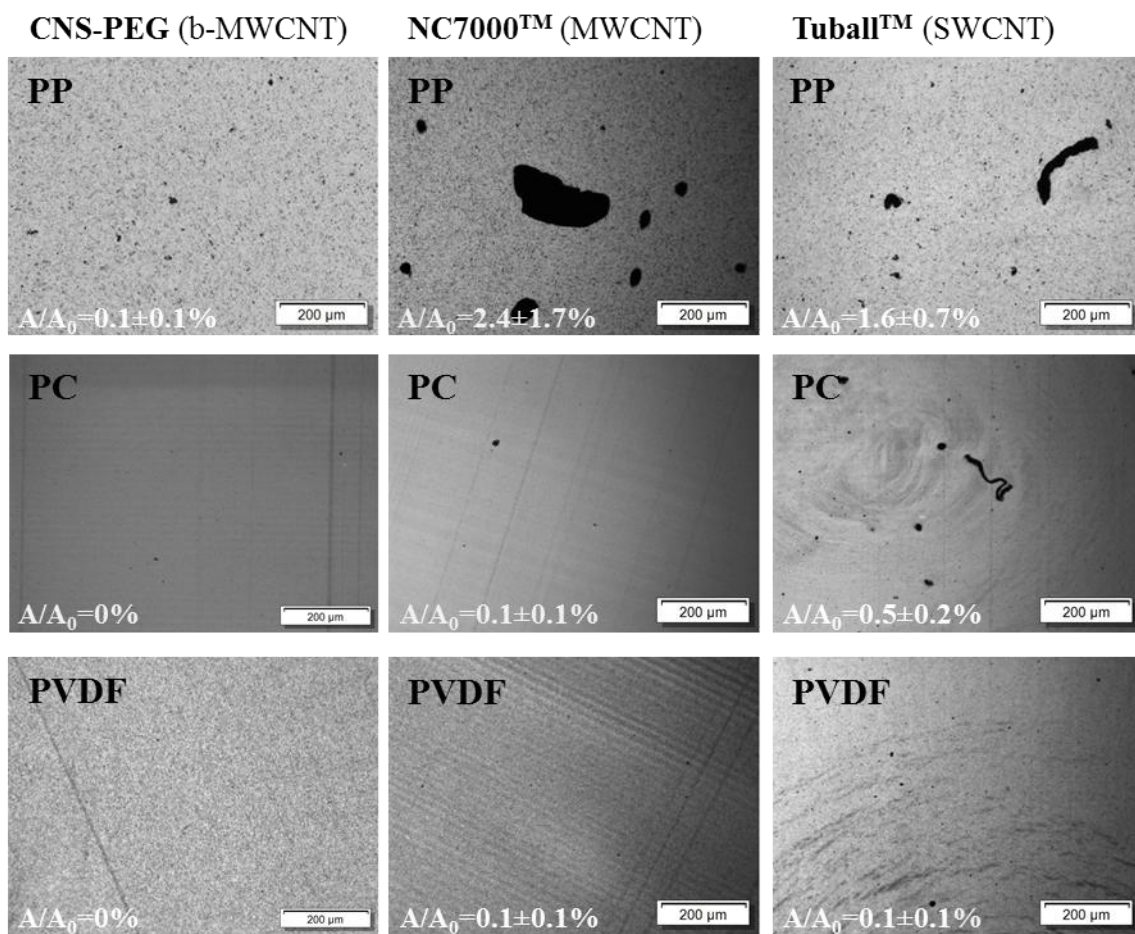


Figure 4 – TEM images of PVDF composite containing 1 wt.-% of the different fillers: (a) CNS-PEG, (b) NC7000™ (b), and (c) Tuball™



Figures 5 – LM images of PP, PC and PVDF composites filled with 1 wt.-% CNS-PEG, NC7000TM or TuballTM

To quantify the state of macrodispersion, transmission light microscopy (LM) was performed on composites with 1 wt.-% CNTs in the different matrices, shown in Figure 5. The PVDF composites are nearly free of visible agglomerates, and the agglomerate area ratios are below 0.1%. . The dispersion is much better than that reported by Ke et al. [66, 72, 73] for PVDF/MWCNT composites using a similar loading of either MWCNTs of the Nanocyl NC3150 series or MWCNTs provided by Chengdu (P.R. China). For PP and PC composites, different sizes and numbers of agglomerates are visible when using the different nanotube materials, which could be quantified by the agglomerate area ratio A/A_0 . For PC, addition of CNS-PEG and NC7000TM results in composites nearly free of agglomerates. For PP, addition of these filler materials leads to very small agglomerates (mostly below the set threshold) in the case of CNS-PEG, but to large spherical agglomerates when using NC7000TM. For both PP and PC, the typical worm-like shapes of TuballTM agglomerates are seen together with some smaller spherical ones. These structures are larger in PP than in PC. The highest agglomerate area ratio was for PP/NC7000TM (2.4 %), indicating the worst macrodispersion among all composites.

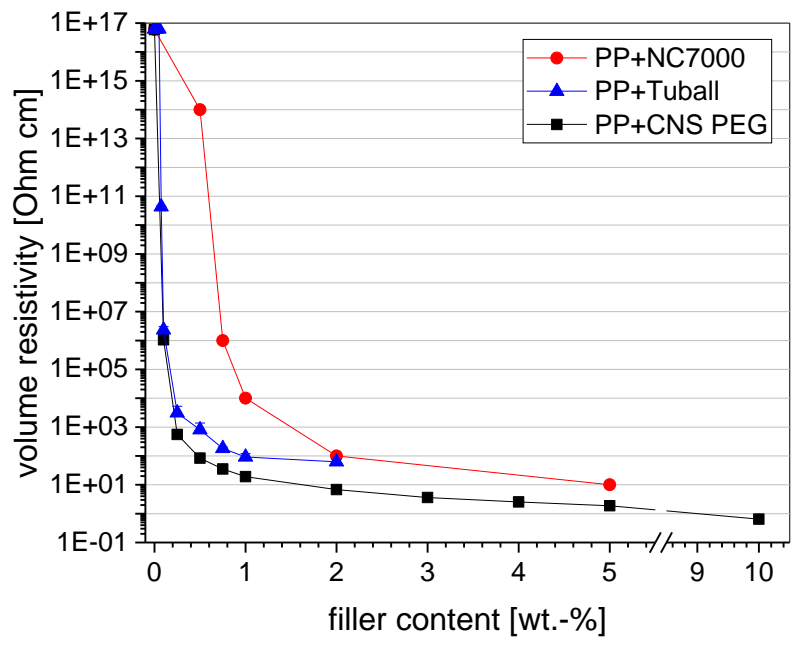
In comparison with previous works, we report better macrodispersion. For the same type of PP and mixing conditions as used in this study, the addition of SWCNTs synthesized by Fraunhofer IWS, Germany resulted in an agglomerate area ratio (determined under the same conditions) of around 5% [22, 65], which exceeds all values measured in this study. For PC-based composites with the same grade of PC, comparisons with MWCNTs of the type NC7000TM and Baytubes[®] are available. Krause et al. [74] reported for a PC/ 2 wt.-% NC7000TM composite (A/A_0 of 1.0%) a better CNT macrodispersion than for a PC/ 2 wt.-%

Baytubes[®] grade C150P composite having agglomerate area ratios, A/A_0 , of 1.8% using the same melt mixing conditions as in present study. For PC filled with 0.75 wt.-% NC7000[™] composite, a nearly agglomerate-free macrodispersion (A/A_0 of $0.1\pm 0.1\%$) was described by Carval et al. [75], which is comparable with results shown in Fig. 5. When using the Baytubes[®] grade C150HP, Kasaliwal et al. [35] described worse MWCNT dispersion, indicated by higher agglomerate area ratios A/A_0 of about 2%. Socher et al. [38] reported for the MWCNT grade Baytubes[®] C150P agglomerate area ratios A/A_0 of $0.2\pm 0.1\%$ when mixed under the same conditions as in this study, which is in the same range as the values reported here for PC/MWCNT NC7000[™] and PC/SWCNT Tuball[™].

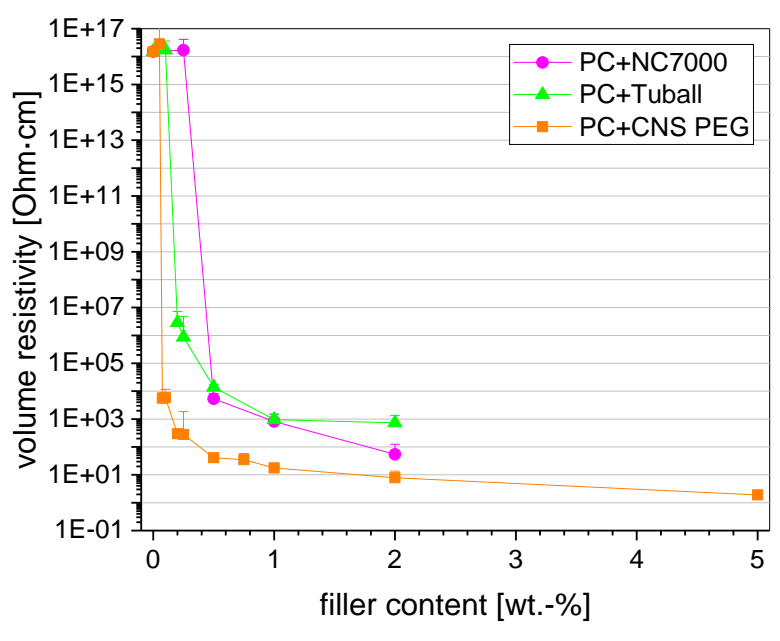
In summary, the best dispersion and distribution in the different matrices at the macroscale was obtained for the branched MWCNTs, namely CNS-PEG. This finding of better dispersability of b-CNTs compared to non-branched follows the outcome of the study of Malik et al. [54], who described a worse dispersability of linear MWCNTs Baytubes[®] C150P in ethanol compared to branched MWCNTs that were prepared by a method for unzipping and re-rolling Baytubes[®] C150P. It is highly remarkable that the branched MWCNTs CNS-PEG exhibit excellent dispersability in all the polymer matrices, even if they have different polarities. Whereas PP is nonpolar, PVDF and PC present more polar structures. The surface properties of the branched MWCNTs lead to good dispersion in all three matrices. It can be assumed that the branched structure itself is a reason for the good dispersability. The high number of branches leads to a porous web-like structure having hollow spaces that would make it easier for the polymer chains to infiltrate into the initial CNT agglomerates. The branched CNTs also stick together less than linear CNTs due to the steric hindrance and possibly also because of the PEG coating.

3.3. Electrical properties of the composites

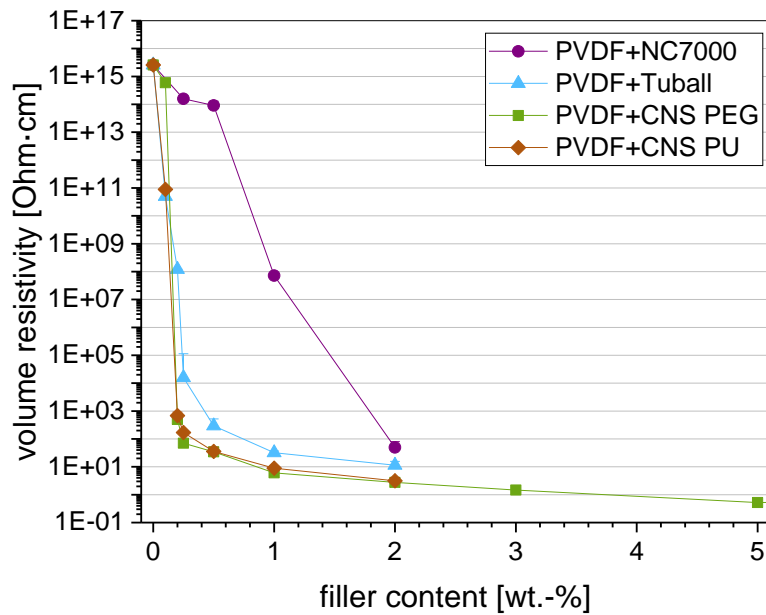
The electrical percolation curves of the different nanotubes in the composites based on PP, PC, and PVDF are presented in Figure 6a-c. For the PP composites (see Fig. 6a), the lowest electrical percolation threshold was found for PP/CNS-PEG composites at < 0.1 wt.-% and for those filled with SWCNTs Tuball™™, percolation occurred between 0.075 and 0.1 wt.-% [20]. For PP composites containing MWCNTs Nanocyl NC7000™, the electrical percolation threshold was observed to be between 0.5 and 0.75 wt.-%. For loadings of 0.25 wt.-% and above, the composites with CNS-PEG have lower resistivity than the composites containing Tuball™ and Nanocyl NC7000™ nanotubes. At higher CNT loadings, PP/CNS-PEG composites show very low volume resistivity values and reach values of about 2 and 0.6 Ohm·cm at 5 wt.-% and 10 wt.-%, respectively. To achieve an electrical resistivity of 10 Ohm·cm, a loading of only 2 wt.-% CNS-PEG was necessary, compared to 5 wt.-% of Nanocyl NC7000™. Other authors [12-17] studied melt-mixed PP composites containing different kinds of multiwalled CNTs and determined higher electrical percolation thresholds (between 0.5 and 3 wt.-%) than for PP/CNS-PEG or PP/Tuball™ composites. Only Andrews et al. [76] reported a comparable low electrical percolation threshold of 0.05 vol% (approx. 0.14 wt.-%) for PP/MWCNT composites prepared by shear mixing in a Haake PolyLab Rheomix compounder. In this study, custom-synthesized MWCNTs with tube diameters in the range 20 to 30 nm and tube lengths of 20 to 100 μm were used, and percolation was studied using surface resistivity measurements on pressed films.



(a)



(b)



(c)

Figure 6 – Volume resistivity of CNT composites for different filler CNT types and loadings:

(a) PP composites, (b) PC composites; (c) PVDF composites

For PC-based composites (Fig. 6b), the lowest electrical percolation threshold of 0.05-0.075 wt.-% was again found when using the filler CNS-PEG. Such a low electrical percolation threshold has not been described before in the literature for a PC matrix. For PC composites filled with SWCNT Tuball™ or MWCNT NC7000™, significantly higher electrical percolation thresholds of 0.1-0.2 wt.-% or 0.25-0.5 wt.-% were observed. The electrical percolation thresholds of the PC composites correlate well with the CNT aspect ratio of the nanotubes, which is highest for CNS-PEG, followed by SWCNT Tuball™ and MWCNT NC7000™. This finding is in agreement with the studies of Castillo et al. [33] and Guo et al. [37] combining different CNT grades (including MWCNT NC7000™) with the same grade of PC under slightly different mixing conditions. In the study of Castillo et al. [33], MWCNT NC7000™ showed a percolation threshold of 0.28 wt.-%. The study by Guo et al. [37] also addresses the effect of shortening the nanotubes during the mixing process, which must be considered for all melt-mixing processes. It was shown that for very long nanotubes, the

initially longer MWCNTs (aspect ratio of 474) are shortened to about the same length as initially shorter ones (aspect ratio of 313), which in that case resulted in comparable percolation thresholds of 0.2 wt.-% [37]. Interestingly, reduction of the mixing time (from 5 to 2.5 min) reduced the percolation threshold to 0.07 wt.-% for both MWCNT types. For melt-mixed PC/MWCNT composites prepared with different nanotubes or PC grades, or mixing conditions differing from those used in our study, other authors reported electrical percolation thresholds of around 0.75 wt.-% [38], 0.5 wt.-% [39], 0.5-1 wt.-% [31, 36], 0.875-1 wt.-% [30], 1-1.5 wt.-% [27-30], and lower than 2 wt.-% [40], which are all higher than the values achieved in this study for PC composites filled with CNS-PEG or SWCNT Tuball™. As found in this study for PP-based composites, the values of volume resistivity at higher loadings are very low for PC/CNS-PEG composites. At 2 wt.-% loading, a value of 8 Ohm·cm was measured for PC/CNS-PEG in comparison to 738 or 54 Ohm·cm for composites with Tuball™ or NC7000™, respectively.

In PVDF-based composites (Fig. 6c) the highest percolation threshold at 1 wt.-% loading was found for the filler MWCNT NC7000™. Significantly lower electrical percolation thresholds were measured for the other fillers, which are in the range of 0.1-0.2 wt.-%. Thereby, CNS-PEG and CNS-PU show at 0.2 wt.-% lower resistivity values than Tuball™. Comparing both modifications of CNS, only at 0.1 wt.-% loading can differences be found. At this concentration, CNS-PU as filler results in reduced resistivity values, whereas CNS-PEG is still non-conductive. At higher loadings the values are nearly identical for both CNS types. At 2 wt.-%, a resistivity value of 2 Ohm·cm was reached for PVDF/CNS in comparison to 11 or 50 Ohm·cm for PVDF/Tuball™ or PVDF/NC7000™, respectively. No previous percolation threshold values using the same nanotubes were found for comparison. When applying the same grade of PVDF but other nanotubes, Ke at al. found for MWCNT Nanocyl NC3150™ melt-mixed under the same conditions as in our study electrical percolation at 0.53 wt.-%

[43], and higher percolation thresholds were described for functionalized MWCNT at 0.60 wt.-% (amino- or hydroxyl-functionalized Nanocyl NC3152TM or NC5153TM) and 0.82 wt.-% (carboxyl-functionalized Nanocyl NC3151TM) [66]. Using another grade of PVDF, Ameli et al. [44] reported electrical percolation between 1 and 2 wt.-% when filled with nitrogen-doped MWCNTs. Arjmand et al. [45] showed for composites containing laboratory-synthesized MWCNTs percolation at around 0.4 wt.-%. In another study, Ke et al. reported for melt-mixed PVDF (different grade)/MWCNT (Chengdu Organic Chemistry) composites electrical percolation between 2 and 3 wt.-% [46]. Using the same MWCNTs as in [46] and applying a two-step processing strategy combining solution and melt compounding, Xiao et al. [77] reported conductivity values of 0.84 S/m (resistivity 11.9 Ohm·cm) for Kynar720/2% MWCNT composites. Arjmand et al. [45] measured electrical conductivity of 6.25 S/cm (resistivity 0.2 Ohm·cm) for PVDF (different grade) with 3.5 wt.-% of laboratory-synthesized MWCNTs.

In summary, the comparison of the electrical percolation thresholds in all three different polymers shows that the lowest percolation threshold always occurs for the branched CNS material and the highest one for MWCNT NC7000TM.

One reason for this finding could be because the **CNT length or rather the aspect ratio** is significantly higher for the CNS material than for Nanocyl NC7000TM. The aspect ratio has an inversely proportional correlation with the percolation threshold in composites [78, 79], and longer CNTs result in lower percolation thresholds. With an initial aspect ratio of around 130, MWCNT NC7000TM has the lowest value among the investigated nanotube materials, correlating with the highest electrical percolation threshold. A 24-times higher initial aspect ratio compared to NC7000TM was stated for SWCNT TuballTM, and a 38-times higher one for CNS-PEG and CNS-PU. Even if in SWCNT materials only a part of the nanotubes are

conductive and contribute to the electrical percolation network, this significantly higher aspect ratio correlates well with the lower electrical percolation threshold compared to NC7000™. However, such discussion of the correlation between aspect ratio and the electrical percolation threshold is only appropriate for linear, non-branched fillers, and when considering the reduction of the aspect ratio during processing, which was not done in our study. As nanotubes mainly break at defects, the shortening characteristics may depend not only on mixing conditions (shear stresses) but may also vary for different types of CNTs. Whereas for MWCNT based composites, studies about the nanotube shortening are available for selected systems [32, 38, 64], no studies are known about the behavior of SWCNTs. Furthermore, the values of **electrical conductivity of different CNT powdery materials** showed differences among the three kinds of nanotubes. The branched CNT structures, namely CNS nanotubes, had the highest values of 33 S/cm (CNS-PEG) and 28 S/cm (CNS-PU) compared to Tuball™ with 14 S/cm and NC7000™ with 15 S/cm. However, these differences cannot entirely explain the large differences in the electrical percolation thresholds of the different nanotubes, as the powder conductivity of the filler does not necessarily scale with the composite conductivity. For example, in composites of polyamide 6.6 with different MWCNTs, for which the powder conductivity values varied between 4 and 30 S/cm, irrespective of these differences, comparable electrical percolation thresholds were found [80].

The **dispersability of the as-produced CNT powders** in the polymeric matrix should also be taken into account. In a study by Pegel et al. [36], different lots of MWCNTs TsNa (Tsinghua-Nafine Nano-Powder Commercialization Engineering Center, Beijing, China) having the same geometrical conditions were used in composites with PC; however for one lot an electrical percolation threshold of around 1 wt.-% was found and for the other percolation between 4 and 5 wt.-%. Similar differences were reported by Krause et al. when

using the same MWCNT lots in polyamide 6.6 [42]. The discrepancies were attributed to the different CNT dispersabilities [70] as indicated by different stabilities of aqueous surfactant dispersions of both TsNa lots. For the PC/TsNa composite having the higher percolation threshold, larger MWCNT agglomerates were found on the nanoscale, illustrating a poorer MWCNT dispersion in the polymer matrix [36].

The **mechanical stability of CNT agglomerates** can be also taken as a measure of their dispersability and can be quantified by the measurement of the breaking or deformation stress of CNT agglomerates. An example is given in [70], where increasing deformation stress of the CNT agglomerates of different CNT materials was taken as measure for the increasing agglomerate strength and could be related to poorer dispersability in aqueous surfactant dispersions. As shown by Krause et al. [42], the dispersability in aqueous surfactant solutions can be related to the dispersion state in a polymer matrix. Thus, CNT materials with high deformation stress also resulted in worse dispersion in the polymer matrix [32, 81, 82]. For example, in polyamide 12 composites, the mechanical stability of the CNT agglomerates (as determined in [70]) correlates with the electrical percolation threshold and CNT dispersion [82]. PA12 composites filled with NC7000™ or FutureCarbon MWCNT (lowest values of CNT deformation stress) had lower electrical percolation threshold and better CNT macro- and nano-dispersion than a PA12 composite containing Baytubes® C150P having a higher value of CNT deformation stress. Ball milling of CNTs leads to densification and a higher CNT agglomerate strength, resulting in PC-based composites with a higher number of remaining CNT agglomerates and a higher electrical percolation threshold [32]. In the present study, only the composites filled with branched CNS-PEG were free of nanotube agglomerates (see Figure 5), illustrating its best dispersability among the three CNT types in all of the investigated matrix materials.

One can further assume that the conductive **network structure** formed during melt mixing differs when using linear or branched CNTs. This is schematically represented in Figure 7. It is generally accepted that conductive networks do not necessarily require direct contacts between neighbored nanotubes and that hopping or tunneling of electrons also allows electrical pathways through an insulating matrix. However, each contact or “quasi-contact” (Fig. 7, red dots) is connected with a contact resistance, reducing the conductivity of the composite [60]. In a network of branched nanotubes, some contact points are already present in the branched nanotube structure, without any resistance losses. Thus, electron transfer can also occur across the junctions (Fig. 7 right) and along the CNT branches. In contrast to linear CNTs, branched CNTs exhibit a two- or even three-dimensional extension, which increases the probability for forming a 3D network. When using nanotubes with a branched structure, higher conductivity values at the same CNT loading may be expected. It can be also assumed that effects of the orientation on the network, as e.g. by stretching of the composite material in when forming films or during melt spinning, are less pronounced in networks based on branched CNT structures. Thus, more stable networks with lower dependence of electrical resistivity on orientation are expected in comparison with networks of linear CNTs.

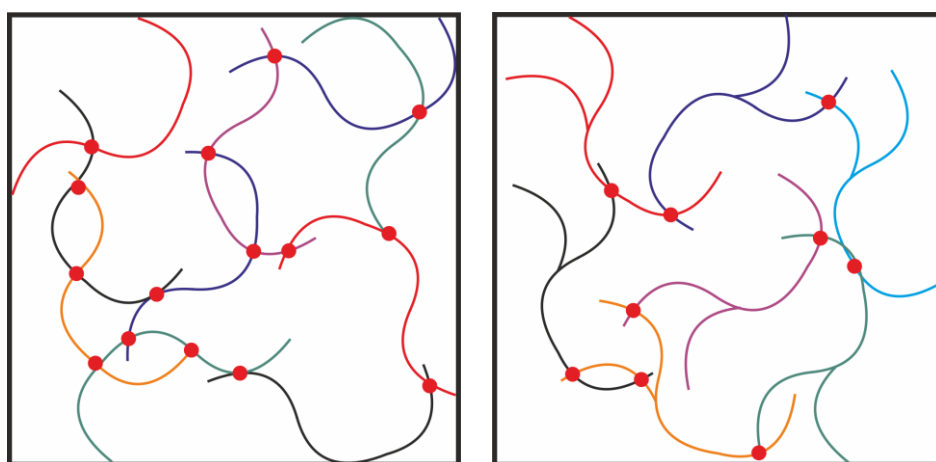


Figure 7 – Schema of network structure in CNT composites for linear (left) and branched (right) nanotubes. The red dots represent the contact points between neighbored nanotubes at which tunneling and hopping processes occur. The schemas contain comparable CNT volume

contents, CNT lengths and diameters (aspect ratio), as well as state of CNT curling. In the network of linear CNTs, many more contact points with high contact resistance are required to form the conductive pathways through the composite compared to network of branched CNTs.

3.4 Thermal conductivity of PP composites

The influence of the different fillers on the thermal conductivity was studied for the PP-based composites (see Table 1). The thermal conductivity of PP (0.28 W/(m·K)) was increased to 0.40 or 0.47 W/(m·K) by incorporating 5 or 10 wt.-% CNS-PEG, respectively. This thermal conductivity is significantly higher than for composites with other MWCNTs (10 wt.-% NC7000™, 0.38 W/(m·K)) or SWCNTs (10 wt.-% SWCNT Fraunhofer IWS, 0.35 W/(m·K)) in the same PP [22]. However, composites filled with Tuball™ achieve significantly higher values compared to CNS-PEG, namely 0.53 and 0.58 W/(m·K) at 5 or 6 wt.-% loading, representing increases of 189 and 202%, respectively. In summary, for increasing the thermal conductivity in PP based composites, the Tuball™ SWCNT material is the best filler choice.

Table 1 - Thermal conductivity of PP composites

sample	Thermal conductivity [W/(m·K)]
PP	0.28±0.01
PP+5 wt.-% CNS-PEG	0.40±0.01
PP+10 wt.-% CNS-PEG	0.47±0.03
PP+10 wt.-% NC7000 [22]	0.38
PP+10 wt.-% SWCNT Fraunhofer IWS [22]	0.35
PP+5 wt.-% Tuball™	0.53±0.01
PP+6 wt.-% Tuball™	0.58±0.04

In comparison, Szentes et al.[12] obtained for a PP/ 5 wt.-% MWCNT NC7000™ composite a much lower thermal conductivity value 0.33 W/(m·K) (corresponding to an increase of 37%

over the pure PP used in their study). Mazov et al. [21] prepared PP/MWCNT composites by a coagulation precipitation technique combined with melt extrusion and observed an increase of thermal conductivity from 0.23 W/(m·K) (pure PP) up to 0.34 W/(m·K) for PP/ 4 wt.-% MWCNT composites. This increase is lower than what we achieved with 5 wt.-% loading of CNS-PEG.

It can be concluded that long CNTs (like in Tuball™ SWCNT), as well as the branched structure (like in CNS-PEG), seem to be favorable for composites with high thermal conductivity. It was expected that the phonon transport, responsible for thermal conduction, occur in branched CNTs more easily than in linear CNTs, due to their branched structures.

3.5 Thermal behavior (DSC) of PP and PVDF composites

The influence of the different types of nanotubes on the thermal behavior of PDVF-based composites was investigated (Table 2). PP/CNS-PEG composites were also studied (Fig. 8). For PP-based composites, a slight increase in the melting temperature, T_m , (160.8 °C for pure PP, 166.1 °C for 10 wt.-% PEG-CNS loading) and a significant increase of the crystallization temperatures, $T_{c,onset}$ and $T_{c,max}$, compared with pure PP were observed (Fig. 8). The relatively large increase in crystallization temperatures of 16 K (10 wt.-% CNS-PEG in PP) implies that the CNTs are well-dispersed, as the ability of CNTs to serve as nuclei depends on the available surface area. In accordance with results of other authors [25, 83-85], the crystallization temperatures of the PP composites rise strongly at low MWCNT contents (0.5-1 wt.-%) followed by levelling off at higher MWCNT contents. The overall crystallinity, α , increases marginally with CNS-PEG addition, from 51% (pure PP) up to 53% for PP/10 wt.-% CNS-PEG. For comparison, Grugel et al. [86] described an increase in $T_{c,onset}$ and $T_{c,max}$ of 7.4 K for PP containing 2 wt.-% MWCNT NC7000™, whereas in our work, the incorporation of only 1 wt.-% CNS-PEG in PP resulted in an increase of 11.6 K and 10.2 K, respectively.

The increase of crystallinity from 46% (pure PP) up to 48% (PP/2 wt.-% NC7000TM) [86] was in the same range as results shown in Fig. 8. In previous investigations using the same conditions for composite preparation, the nucleation behavior was even more pronounced when using SWCNT TuballTM [20]. For PP with only 2 wt.-% SWCNT TuballTM, increases of $T_{c, \text{onset}}$ and $T_{c, \text{max}}$ by 17.1 K and 16.0 K, respectively, were measured. These increases are higher than in comparable systems with other nanoscaled carbon fillers. Gärtner et al. [22] found an increase in $T_{c, \text{onset}}$ and $T_{c, \text{max}}$ of 7.4 and 8.8 K for PP containing 2 wt.-% SWCNT (producer Fraunhofer IWS). Jeon et al. [23] studied PP with purified SWCNT HiPco and also found a large increase by 13 K in crystallization temperatures upon 1 wt.-% SWCNT addition. Valenti et al. [25] investigated the thermal properties of melt-mixed PP composites with 5 wt.-% SWCNT CarboLex and observed an increase in $T_{c, \text{max}}$ from 101°C to 114°C. In [20], an increase in the melting temperature from 160.8 °C to 167.0 °C was reported when SWCNT TuballTM (2 wt.-%) were incorporated in PP, which is comparable to the present study.

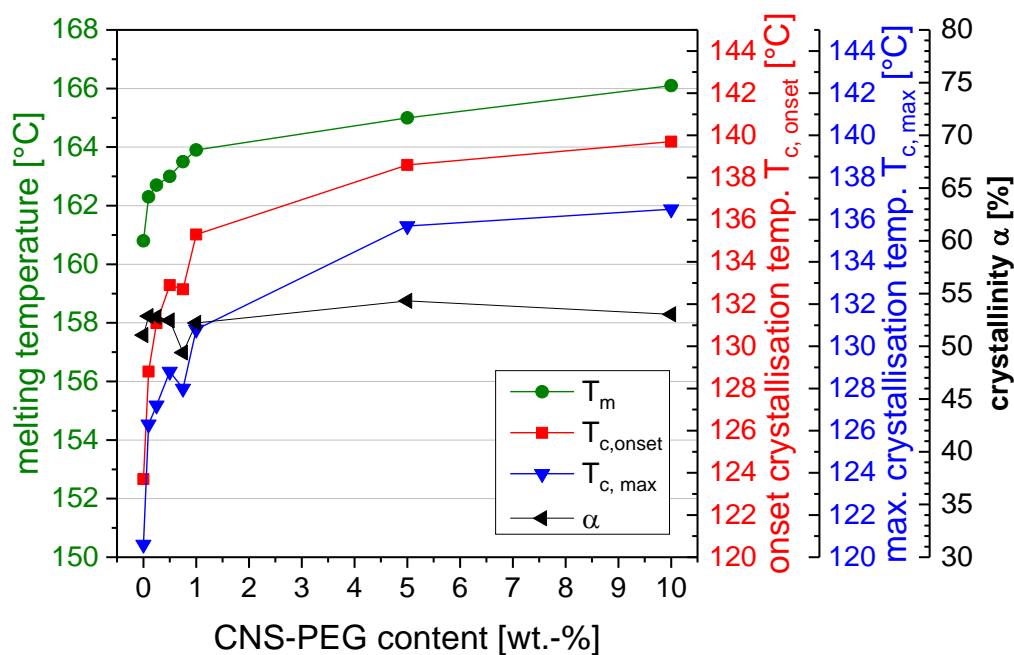


Figure 8 – Thermal behavior of PP/CNS-PEG composites: typical values obtained from DSC vs. the CNS-PEG content

In the PVDF composites (Table 2), the incorporation of all three kinds of CNTs leads to significant increases of the crystallization temperatures ($T_{c, \text{onset}}$, $T_{c, \text{max}}$) and a marginal increase of the melting temperatures, T_m . The increases in the crystallization temperatures were more pronounced for SWCNT Tuball™ and b-MWCNT CNS-PEG, with increases of 6 K for PVDF composites containing 2 wt.-% filler. In contrast, addition of 2 wt.-% NC7000™ leads to an increase of only 4 K. This finding is in good agreement with results of Ke et al. [46, 66, 73, 87] for PVDF composites with MWCNT materials from Nanocyl having different functionalities. For PVDF based composites, the crystallization temperatures start to plateau at 1 wt% filler. The crystallinity of the PVDF decreases slightly with the incorporation of all kinds of CNTs (Table 2), and this effect is more pronounced for PVDF/NC7000™ composites. Among the three CNT types, the PVDF composites with CNS-PEG show the lowest decrease of crystallinity (from 75.0% to values between 69.4-71.5%). In the literature, for PVDF (another type than used here) with 2 wt.-% MWCNT (Chengdu, China) prepared by a two-step processing strategy combining solution and melt compounding, a crystallinity decrease from 34.3% to 32.7% and crystallization temperature increase from 139.3 to 148.1 °C were reported, whereas the melting temperature was unchanged [77]. This illustrates that a slightly decrease in crystallinity seems to be a common phenomenon for PVDF upon CNT incorporation.

Table 2 - Thermal behavior of PVDF composites containing SWCNT Tuball™, MWCNT NC7000™ or branched MWCNT CNS-PEG: values obtained from DSC

	T_m [°C]	$T_{c, \text{onset}}$ [°C]	$T_{c, \text{max}}$ [°C]	crystallinity α [%]
--	---------------	-------------------------------	-----------------------------	-------------------------------

PVDF processed	168.6	142.7	140.8	75.0
PVDF+0.1% Tuball	168.9	146.4	144.5	70.0
PVDF+0.25% Tuball	169.9	147.6	145.7	68.6
PVDF+0.5% Tuball	171.2	147.8	145.2	68.7
PVDF+1% Tuball	169.5	148.3	146.7	71.0
PVDF+2% Tuball	169.5	148.6	146.9	68.9
PVDF+0.25% NC7000	169.0	145.2	143.0	67.1
PVDF+0.5% NC7000	168.6	146.1	144.1	67.8
PVDF+1% NC7000	168.1	146.6	144.9	67.4
PVDF+2% NC7000	169.9	146.7	144.3	66.7
PVDF+0.1% CNS-PEG	168.6	146.6	144.2	71.4
PVDF+0.25% CNS-PEG	168.3	148.3	146.7	70.3
PVDF+0.5% CNS-PEG	169.5	148.4	146.4	69.4
PVDF+1% CNS-PEG	167.5	149.0	147.7	71.0
PVDF+2% CNS-PEG	170.0	148.9	146.6	71.5

4. Summary

In this study, linear SWCNT Tuball™ and MWCNT NC7000™, as well as branched MWCNT CNS-PEG and CNS-PU, were incorporated in PP, PVDF and PC by melt mixing using a small-scale microcompounder. In all three matrices, the branched MWCNTs CNS-PEG were well dispersed, as shown by transmission light microscopy investigations on thin sections. For all three matrix materials, composites with 1.0 wt.-% loading were free of agglomerates. This is a highly remarkable result, because the three polymer types have very different polarities with PC and PVDF being polar and PP, nonpolar. This indicates that the surface properties of these branched CNTs are quite versatile and provide suitable wetting by the different polymers. The dispersability of this material is excellent, irrespective of the polymer matrix.

The branched MWCNT CNS-PEG provides the best electrical properties in all three polymer matrices. In PP, the electrical percolation threshold of <0.1 wt.-% b-MWCNTs is extremely low for MWCNTs in nonpolar polymers. At higher loadings, very low resistivity values (as compared to other PP-based composites) can be achieved; these values are as low as about 10

Ohm·cm at 2 wt.-% loading and 2 Ohm·cm at 5 wt.-% loading. The same low electrical percolation threshold was found for SWCNT Tuball™ material in PP. However, for these SWCNTs, the resistivity values at higher filler content were higher than for PP/CNS-PEG composites. For PC- and PVDF-based composites, very low electrical percolation thresholds of PC/CNS-PEG at 0.05-0.075 wt.-% and PVDF filled with CNS-PEG, CNS-PU, or SWCNT Tuball™ at 0.1-0.2 wt.-% were measured, which have not been described before in the literature for melt-mixed composites. In this comparison, the composites containing MWCNT NC7000™ always resulted in the highest electrical percolation threshold and volume resistivity values. This can be explained by the much lower aspect ratio of MWCNT NC7000™ compared to the other two fillers. The branched MWCNT, however, appears to more easily form a stable conductive network due to the existence of junctions at branching points compared to the linear CNTs.

For increasing the thermal conductivity in PP composites the use of Tuball™ SWCNT is the best choice; at 6 wt.-% loading, values of 0.58 W/(m·K) were achieved, compared to 0.28 W/(m·K) for pure PP.

The study of the thermal behavior of both PP- and PVDF-based composites exhibited a significant increase in crystallization temperatures and a marginal increase in melting temperature, which was found for all three CNT types. Thereby, these effects were more pronounced for branched CNS-PEG and SWCNT Tuball™, as compared to MWCNT NC7000™. The high increases in the crystallization temperatures (up to 16 K @ 10 wt.-% CNS-PEG loading in PP and 6 K @ 2 wt.-% Tuball™ or CNS-PEG loading in PVDF) also indicate that good nanotube dispersion was achieved, because the nucleation efficiency depends on the amount of the available surface of nanotubes.

The branched MWCNT material appears to be highly suitable for use in melt-mixed composites, especially for electrical applications. In future work, the mechanical properties of

such composites will be studied. It may be expected that the branched structure also causes improved interactions between the nanotubes and polymer chains, combined with increased interfacial bonding with the polymer matrix.

Acknowledgement

The authors thank Applied NanoStructured Solutions, LLC (USA) for providing the CNS-PEG and CNS-PU material and SEM (Fig. 1b) and TEM micrographs (Fig. 2 right). The authors also appreciate the help of Mrs. M. Heber in TEM and SEM and of Mrs. L. Häußler and Mrs. K. Arnold in DSC measurements (all from IPF).

References

1. Alig I, Pötschke P, Lellinger D, Skipa T, Pegel S, Kasaliwal GR, and Villmow T. *Polymer* 2012;53(1):4-28.
2. Sathyanarayana S and Hübner C. Thermoplastic Nanocomposites with Carbon Nanotubes. In: Njuguna J, editor. *Structural Nanocomposites*. Berlin Heidelberg: Springer-Verlag, 2013. pp. 19-60.
3. Byrne MT and Gun'ko YK. *Advanced Materials* 2010;22(15):1672-1688.
4. Bauhofer W and Kovacs JZ. *Composites Science and Technology* 2009;69(10):1486-1498.
5. Qiang L and Baidurya B. *Nanotechnology* 2005;16(4):555.
6. David Tn. *Journal of Physics: Condensed Matter* 2005;17(13):R413.
7. Ma W, Miao T, Zhang X, Yang L, Cai A, Yong Z, and Li Q. *Carbon* 2014;77:266-274.
8. Kim P, Shi L, Majumdar A, and McEuen PL. *Physical Review Letters* 2001;87(21):215502.
9. Xiao-Wu T, Yong Y, Woong K, Qian W, Pengfei Q, Hongjie D, and Lei X. *Physics in Medicine and Biology* 2005;50(3):N23.
10. .
11. Seo M-K and Park S-J. *Chemical Physics Letters* 2004;395(1-3):44-48.
12. Szentés A, Varga C, Horvath G, Bartha L, Konya Z, Haspel H, Szel J, and Kukovecz A. *eXPRESS Polymer Letters* 2012;6(6):494-502.
13. Müller MT, Krause B, Kretzschmar B, and Pötschke P. *Composites Science and Technology* 2011;71(13):1535-1542.
14. Zhong J, Isayev AI, and Huang K. *Polymer* 2014;55(7):1745-1755.
15. Hwang TY, Kim HJ, Ahn Y, and Lee JW. *Korea-Australia Rheology Journal* 2010;22(2):141-148.
16. Menzer K, Krause B, Boldt R, Kretzschmar B, Weidisch R, and Pötschke P. *Composites Science and Technology* 2011;71(16):1936-1943.
17. Mičušík M, Omastová M, Krupa I, Prokes J, Pissis P, Logakis E, Pandis C, Pötschke P, and Pionteck J. *Journal of Applied Polymer Science* 2009;113(4):2536-2551.
18. Andrews R, Jacques D, Minot M, and Rantell T. *Macromolecular Materials and Engineering* 2002;287(6):395-403.
19. Narimani A and Hemmati M. *Polymers & Polymer Composites* 2014;22(6):533-540.
20. Krause B, Pötschke P, Ilin E, and Predtechenskiy M. *Polymer* 2016;98:45-50.

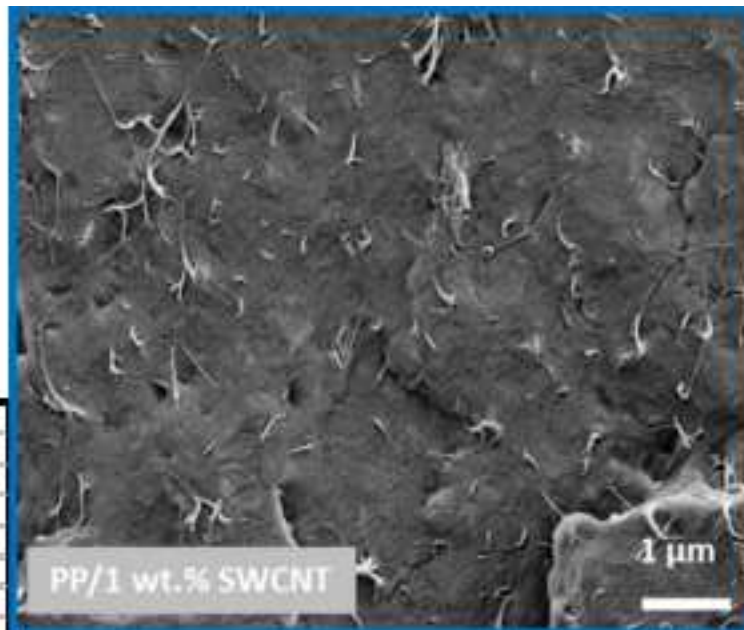
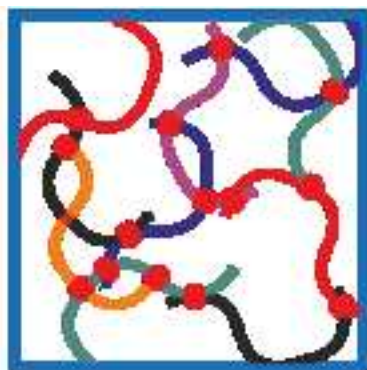
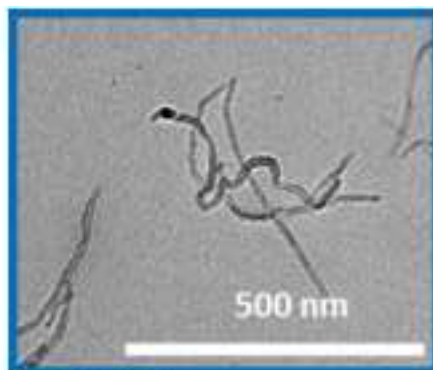
21. Mazov I, Burmistrov I, Il'inykh I, Stepashkin A, Kuznetsov D, and Issi J-P. *Polymer Composites* 2015;36(11):1951-1957.
22. Gärtner T, Pötschke P, and Voit B. New nanostructured carbon materials in melt-mixed PP composites. 6th International Conference on Carbon Nanoparticle based Composites (CNPComp). Dresden, Germany, 2013.
23. Jeon K, Warnock S, Ruiz-Orta C, Kismarahardja A, Brooks J, and Alamo RG. *Journal of Polymer Science Part B: Polymer Physics* 2010;48(19):2084-2096.
24. Leelapornpisit W, Ton-That M-T, Perrin-Sarazin F, Cole KC, Denault J, and Simard B. *Journal of Polymer Science Part B: Polymer Physics* 2005;43(18):2445-2453.
25. Valentini L, Biagiotti J, Kenny JM, and Santucci S. *Journal of Applied Polymer Science* 2003;87(4):708-713.
26. Kasaliwal GR, Gödel A, and Pötschke P. *Journal of Applied Polymer Science* 2009;112(6):3494-3509.
27. Pötschke P, Dudkin SM, and Alig I. *Polymer* 2003;44(17):5023-5030.
28. Pötschke P, Bhattacharyya AR, Janke A, and Goering H. *Composite Interfaces* 2003;10(4-5):389-404.
29. Sadhu VB, Pionteck J, Pötschke P, Jakisch L, and Janke A. *Macromolecular Symposia* 2004;210:165-174.
30. Pötschke P, Bhattacharyya AR, and Janke A. *Carbon* 2004;42(5-6):965-969.
31. Lin B, Sundararaj U, and Pötschke P. *Macromolecular Materials and Engineering* 2006;291(3):227-238.
32. Krause B, Villmow T, Boldt R, Mende M, Petzold G, and Pötschke P. *Composites Science and Technology* 2011;71(8):1145-1153.
33. Castillo FY, Socher R, Krause B, Headrick R, Grady BP, Prada-Silvy R, and Pötschke P. *Polymer* 2011;52(17):3835-3845.
34. Kasaliwal GR, Pegel S, Gödel A, Pötschke P, and Heinrich G. *Polymer* 2010;51(12):2708-2720.
35. Kasaliwal GR, Gödel A, Pötschke P, and Heinrich G. *Polymer* 2011;52(4):1027-1036.
36. Pegel S, Pötschke P, Petzold G, Alig I, Dudkin SM, and Lellinger D. *Polymer* 2008;49(4):974-984.
37. Guo J, Liu Y, Prada-Silvy R, Tan Y, Azad S, Krause B, Pötschke P, and Grady BP. *Journal of Polymer Science Part B: Polymer Physics* 2014;52(1):73-83.
38. Socher R, Krause B, Müller MT, Boldt R, and Pötschke P. *Polymer* 2012;53(2):495-504.
39. Pötschke P, Zschoerper NP, Moller BP, and Vohrer U. *Macromolecular Rapid Communications* 2009;30(21):1828-1833.
40. Kim J and Son Y. *Polymer* 2016;88:29-35.
41. Zhang Z, Peng K, and Chen Y. *eXPRESS Polymer Letters* 2011;5(6):516-525.
42. Krause B, Petzold G, Pegel S, and Pötschke P. *Carbon* 2009;47(3):602-612.
43. Ke K, Pötschke P, Wiegand N, Krause B, and Voit B. *ACS Applied Materials & Interfaces* 2016;8(22):14190-14199.
44. Ameli A, Arjmand M, Pötschke P, Krause B, and Sundararaj U. *Carbon* 2016;106:260-278.
45. Arjmand M and Sundararaj U. *Composites Science and Technology* 2015;118:257-263.
46. Ke K, Wang Y, Zhang K, Luo Y, Yang W, Xie B-H, and Yang M-B. *Journal of Applied Polymer Science* 2012;125(S1):E49-E57.
47. Georgousis G, Pandis C, Kalamiotis A, Georgiopoulos P, Kyritsis A, Kontou E, Pissis P, Micusik M, Czanikova K, Kulicek J, and Omastova M. *Composites Part B: Engineering* 2015;68:162-169.
48. Sun Y-C, Terakita D, Tseng AC, and Naguib HE. *Smart Materials and Structures* 2015;24(8):085034.
49. Meng G, Jung YJ, Cao A, Vajtai R, and Ajayan PM. *Proceedings of the National Academy of Sciences of the United States of America* 2005;102(20):7074-7078.
50. Jin C, Suenaga K, and Iijima S. *Nat Nano* 2008;3(1):17-21.
51. Terrones M, Terrones H, Banhart F, Charlier JC, and Ajayan PM. *Science* 2000;288(5469):1226.

52. Raghuvver MS, Ganesan PG, D'Arcy-Gall J, Ramanath G, Marshall M, and Petrov I. *Applied Physics Letters* 2004;84:4484.
53. Joh H-I, Ha HY, Prabhuram J, Jo SM, and Moon SH. *Carbon* 2011;49(13):4601-4603.
54. Malik S, Nemoto Y, Guo H, Ariga K, and Hill JP. *Beilstein Journal of Nanotechnology* 2016;7:1260-1266.
55. AuBuchon JF, Chen L-H, Daraio C, and Jin S. *Nano Letters* 2006;6(2):324-328.
56. Du GH, Li WZ, Liu YQ, Ding Y, and Wang ZL. *The Journal of Physical Chemistry C* 2007;111(39):14293-14298.
57. Gothard N, Daraio C, Gaillard J, Zidan R, Jin S, and Rao AM. *Nano Letters* 2004;4(2):213-217.
58. Wei D, Liu Y, Cao L, Fu L, Li X, Wang Y, Yu G, and Zhu D. *Nano Letters* 2006;6(2):186-192.
59. Ling L, Lin Z, and Jim L. *Applied Physics Letters* 2012;101:161907.
60. Nirmalraj PN, Lyons PE, De S, Coleman JN, and Boland JJ. *Nano Letters* 2009;9(11):3890-3895.
61. Fu S, Zhou B, and Lung C. *Composites Science and Technology* 1993;47(3):245-250.
62. Suzuki T, Miyajima T, and Sakai M. *Composites Science and Technology* 1994;51(2):283-289.
63. Müller MT, Krause B, and Pötschke P. *Polymer* 2012;53(15):3079-3083.
64. Krause B, Boldt R, and Pötschke P. *Carbon* 2011;49(4):1243-1247.
65. Flaris V, Pötschke P, Gärtner T, Voit B, Rivas R, and Siccardi H. Characterization of melt mixed PP composites with new nanostructured carbon materials. ANTEC 2015, Technical Conference & Exhibition. Orlando, Florida, USA, 2015.
66. Ke K, Pötschke P, Jehnichen D, Fischer D, and Voit B. *Polymer* 2014;55(2):611-619.
67. Krause B, Boldt R, Häußler L, and Pötschke P. *Composites Science and Technology* 2015;114:119-125.
68. Gaur U and Wunderlich B. *Journal of Physical and Chemical Reference Data* 1981;10(4):1051-1064.
69. Gaur U, Lau Sf, Wunderlich BB, and Wunderlich B. *Journal of Physical and Chemical Reference Data* 1983;12(1):65-89.
70. Krause B, Mende M, Pötschke P, and Petzold G. *Carbon* 2010;48(10):2746-2754.
71. Arjmand M, Chizari K, Krause B, Pötschke P, and Sundararaj U. *Carbon* 2016;98:358-372.
72. Ke K, Wang Y, Liu X-Q, Cao J, Luo Y, Yang W, Xie B-H, and Yang M-B. *Composites Part B: Engineering* 2012;43(3):1425-1432.
73. Ke K, Wang Y, Yang W, Xie B-H, and Yang M-B. *Polymer Testing* 2012;31(1):117-126.
74. Krause B, Mende M, Petzold G, Boldt R, and Pötschke P. *Chemie Ingenieur Technik* 2012;84(3):263-271.
75. Krause B, Carval J, and Pötschke P. *AIP Conference Proceedings* 2017;1914(1):030007.
76. Lee K-Y and Kim K-Y. *Polymer Degradation and Stability* 2008;93(7):1290-1299.
77. Xiao Y-j, Wang W-y, Lin T, Chen X-j, Zhang Y-t, Yang J-h, Wang Y, and Zhou Z-w. *The Journal of Physical Chemistry C* 2016;120(12):6344-6355.
78. Stauffer D and Aharony A. *Introduction in percolation theory*. London: Taylor and Francis, 1994.
79. Balberg I. *Philosophical Magazine Part B* 1987;56(6):991-1003.
80. Krause B, Ritschel M, Täschner C, Oswald S, Gruner W, Leonhardt A, and Pötschke P. *Composites Science and Technology* 2010;70(1):151-160.
81. Krause B, Mende M, Petzold G, Boldt R, and Pötschke P. Characterization of dispersability of industrial nanotube materials and their length distribution before and after melt processing. In: Tasis D, editor. *Carbon Nanotube-Polymer Composites*. Cambridge, UK: Royal Society of Chemistry, 2013. pp. 212-233.
82. Socher R, Krause B, Boldt R, Hermasch S, Wursche R, and Pötschke P. *Composites Science and Technology* 2011;71(3):306-314.
83. Razavi-Nouri M. *Journal of Applied Polymer Science* 2012;124(3):2541-2549.
84. Kaganj AB, Rashidi AM, Arasteh R, and Taghipoor S. *Journal of Experimental Nanoscience* 2009;4(1):21-34.

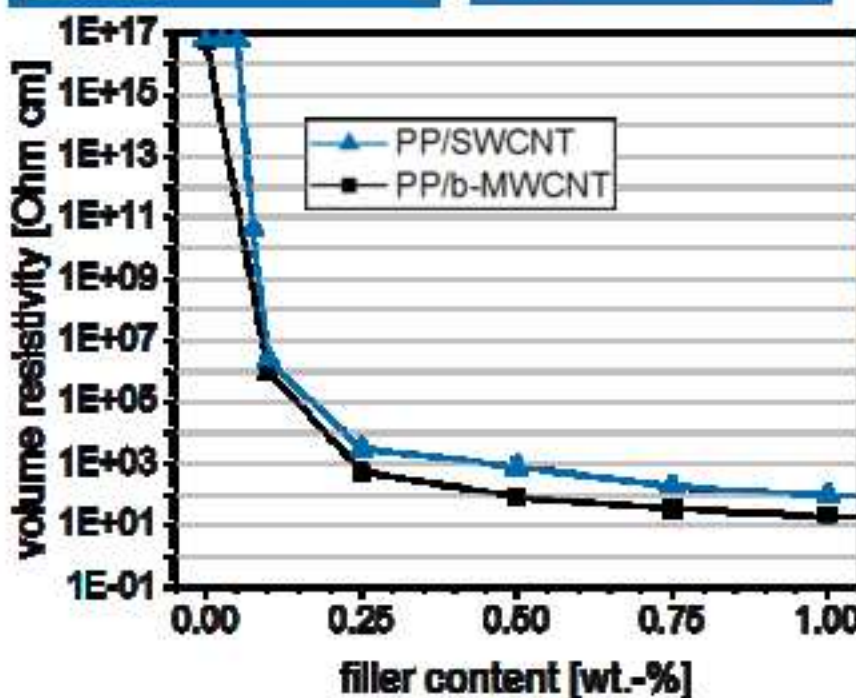
85. Machado MAL, Valentini L, Biagiotti J, and Kenny JM. Carbon 2005;43(7):1499-1505.
86. Grugel F. Untersuchungen zu den Einflussgrößen beim Schmelzecompondieren von Polypropylen-Carbon-Nanotubs-Nanokompositen. Fakultät für Mathematik und Naturwissenschaften, vol. Großer Beleg. Dresden: Technische Universität Dresden, 2012.
87. Ke K, Wen R, Wang Y, Yang W, Xie B-H, and Yang M-B. Journal of Materials Science 2011;46(5):1542-1550.

Highlights

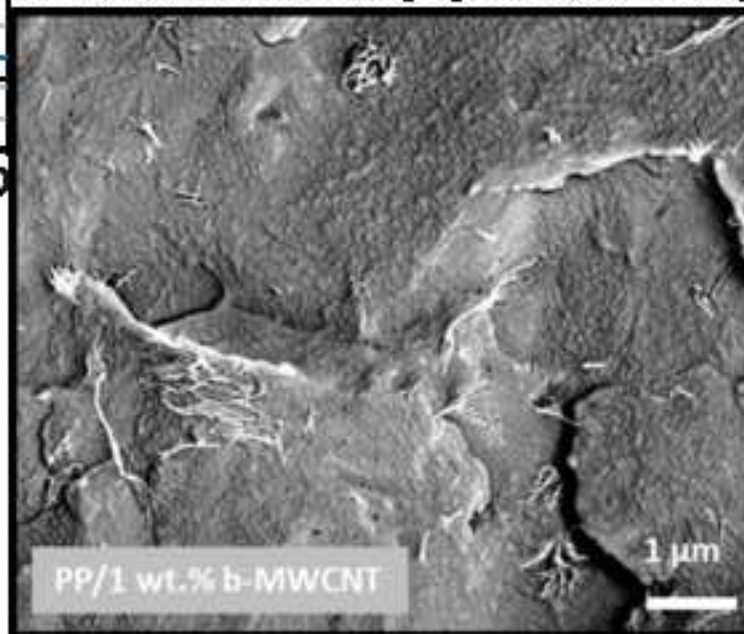
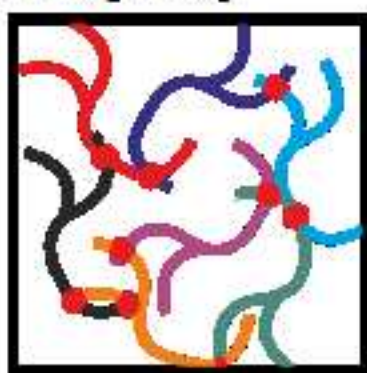
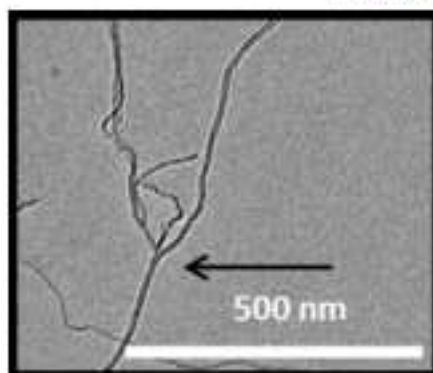
- Comparison of 3 CNT types (SWCNT, MWCNT, branched MWCNT) in PP, PC, and PVDF
- Comparatively best state of dispersion for branched MWCNTs in all matrices
- Electrical percolation < 0.1 wt.-% for PP and PVDF composites with branched MWCNTs
- Highest enhancement in thermal conductivity of PP with SWCNTs
- Crystallization temperature in PVDF most enhanced for SWCNTs



Linear nanotubes (aspect ratio ~3100)



Branched nanotubes (aspect ratio ~5000)



PP/1 wt.% b-MWCNT